Catalysis Today 146 (2009) 285–292

Contents lists available at ScienceDirect

Catalysis Today

journal homepage: www.elsevier.com/locate/cattod

Steady-state multiplicity phenomena during the electrochemical promotion of NO reduction by C_2H_4 in presence of O_2 on thin Rh and Pt catalyst-electrodes in a monolithic electropromoted reactor

S. Souentie *, A. Hammad, C.G. Vayenas

Laboratory of Chemical and Electrochemical Processes (LCEP), Department of Chemical Engineering, University of Patras, Caratheodory 1, GR-26504 Patras, Greece

ARTICLE INFO

Article history:
Available online 31 May 2009

Keywords:
Electrochemical promotion
EPOC
NEMCA effect
NO reduction
Rh catalyst-electrodes
Pt catalyst-electrodes
Steady-state multiplicity

ABSTRACT

The electrochemical promotion of catalysis (EPOC) was used to promote the selective reduction of NO by hydrocarbons in presence of oxygen using thin (~40 nm) porous Rh and Pt catalyst layers sputtered on the opposite surfaces of thin (0.25 mm) solid electrolyte (YSZ) plates serving as electrocatalytic elements of a monolithic electrochemically promoted reactor (MEPR). Using 22 Rh/YSZ/Pt type cells it was found that the reduction of NO in presence of 1.1 kPa O_2 and 0.36 kPa C_2H_4 can be efficiently electropromoted with 340% rate enhancement, reaching 95% NO conversion with 100% selectivity to N_2 in the temperature range from 280 to 340 °C. The apparent Faradaic efficiency is larger than unity for both the NO reduction and the C_2H_4 oxidation reaction.

At elevated temperatures (≥300 °C) and high reactant conversions it was found that after current interruption, the catalytic rates do not return to their initial values but remain in a new highly active steady state. It appears that this highly active state is not a genuine intrinsic permanent NEMCA state but is manifestation of steady-state multiplicity in the monolithic reactor resulting from near complete gaseous O_2 consumption. Thus the low and high activity steady states corresponding to zero applied potential appear to correspond to high and low average P_{O_2} in the reactor. The latter is the result of the near complete reactant conversion under the preceding electropromoted operation. These highly active permanent NEMCA states may be quite useful for practical applications.

© 2009 Elsevier B.V. All rights reserved.

1. Introduction

The electrochemical promotion of catalysis (EPOC) or electropromotion (EP), or non-Faradaic electrochemical modification of catalytic activity (NEMCA effect), is a phenomenon where the application of small currents or potentials on catalysts in contact with solid electrolytes leads to pronounced strongly non-Faradaic and reversible changes in the catalytic activity and selectivity [1–15]. Many studies have shown that electrochemical promotion results from electrochemically controlled migration of promoting ionic species (i.e. $O^{\delta-}$, H^+, $Na^{\delta+}$) from the electrolyte support to the gas exposed catalytic surface [9,13,14] and that classical promotion, electrochemical promotion and metal-support interactions with O^{2-} conducting and mixed ionic–electronic conducting supports are functionally identical and only operationally different [14,16]. Electrochemical promotion allows for in situ control of catalyst activity and selectivity by controlling in situ the promoter coverage via potential application [1–17].

Two parameters are commonly used to quantify the magnitude of electrochemical promotion effect, i.e. the rate enhancement ratio, ρ, and the Faradaic efficiency, Λ [1–5,14]. In the present case of NO reduction by C_2H_4 in presence of O_2 they are defined from:

$$\rho_{CO_2} = \frac{r_{o,CO_2} + \Delta r_{CO_2}}{r_{o,CO_2}}; \quad \rho_{NO} = \frac{r_{o,NO} + \Delta r_{NO}}{r_{o,NO}};$$
$$\Lambda_{CO_2} = \frac{\Delta r_{CO_2}}{I/2F}; \quad \Lambda_{NO} = \frac{\Delta r_{NO}}{I/2F} \tag{1}$$

where r_{CO_2} and r_{NO} (the total rate of consumption of NO) are expressed in mol O and subscript "o" denotes open circuit conditions. In addition to these parameters, when describing electrochemical promotion at high reactants conversions, as in the present case, it is important to define a third parameter, the effective rate enhancement ratio, ρ_c, defined from:

$$\rho_c = \frac{\rho}{\rho_{max}} \tag{2}$$

where ρ_{max} expresses the maximum allowable ρ value due to complete or, more generally, equilibrium conversion.

Reduction of pollutant emissions present in the exhaust of lean-burn and diesel engines has attracted great scientific interest in

* Corresponding author. Tel.: +30 2610 997860; fax: +30 2610 997269.
E-mail address: souentie@chemeng.upatras.gr (S. Souentie).

0920-5861/$ – see front matter © 2009 Elsevier B.V. All rights reserved.
doi:10.1016/j.cattod.2009.04.020

recent years [18–20]. One possible way to achieve high efficiency in this process is the selective catalytic reduction (SCR) of nitrogen oxides by hydrocarbons over noble metal catalysts. Rhodium (Rh) and platinum (Pt) are quite selective catalysts for NO reduction, but under highly oxidizing (i.e. lean-burn) conditions Rh becomes unreactive due to surface Rh_2O_3 formation [21–24], while Pt favors the formation of N_2O at lower temperatures.

The main overall stoichiometric reactions taking place on both Rh and Pt catalyst-electrodes are the following:

$$C_2H_4 + 6NO \rightarrow 2CO_2 + 3N_2 + 2H_2O \quad (3)$$

$$C_2H_4 + 12NO \rightarrow 2CO_2 + 6N_2O + 2H_2O \quad (4)$$

$$C_2H_4 + 3O_2 \rightarrow 2CO_2 + 2H_2O \quad (5)$$

In the present study, the selective catalytic reduction of NO by ethylene in presence of low excess of oxygen was examined using 22 Rh/YSZ/Pt type flat plate cells in a monolithic electrochemically promoted reactor (MEPR), described in detail elsewhere [25–29].

Previous studies have shown that the reduction of NO_x by ethylene in presence of O_2, is a reaction which is electropromoted predominantly by positive applied potential on Rh [30,31] (electrophobic behaviour) and predominantly by negative applied potential on Pt [14,31,32] (electrophilic behaviour). This dictated the choice of Rh and Pt as catalyst-electrodes in the MEP reactor. In this way one expects a synergistic effect of the electropromotion of Rh and Pt deposited on YSZ, when the Rh film is made positive and the Pt film negative.

There have been two recent studies [29,30] of the electropromotion of NO reduction by C_2H_4 utilizing monolithic electropromoted reactors (MEPR). The first one [29] utilized sputtered bimetallic Pt–Rh catalysts and Au counter electrodes, i.e. eight Pt–Rh/YSZ/Au plates and showed electropromotion with positive potentials up to $P_{O_2} = 10$ kPa at 335 °C [29].

The second one [30] utilized, similarly to the present work, 22 Rh/YSZ/Pt plates and studied the MEPR performance under very oxidizing conditions, i.e. $P_{O_2} = 10$ kPa and showed successful and reversible electropromotion with both positive and negative applied potential at temperatures as low as 220 °C. Under these highly oxidizing operating conditions, no irreversibility or steady-state multiplicity phenomena were observed [30].

In the present study we have studied the performance of the same 22 Rh/YSZ/Pt plates used in [30] to study the MEPR performance under near-stoichiometric conditions, i.e. feed P_{O_2} values of 1.1 kPa, because we found that under these conditions very significant permanent electropromotion [4,34,35] and steady-state multiplicity phenomena are observed which appear to be of potential significant practical importance.

Throughout this paper we use the sign convention that the Rh film is the working electrode and the Pt film is the counter electrode so that positive potential, U, implies that the Rh potential is higher than that of the Pt electrode and positive (anodic) applied current corresponds to a flux of $O^{\delta-}$ ions directed from the Pt to the Rh electrode.

It should be noted that both the Rh and Pt films are catalytically active and therefore the measured r_{CO_2} and r_{NO} values correspond to the sum of the rates on the Rh and Pt catalyst films. Therefore the terms "electrophobic", "electrophilic", "volcano" and "inverted volcano" [14] used to describe the observed electropromotion behaviour are used in broad sense, characterizing the electropromotion behaviour of the Rh/YSZ/Pt elements (U is the potential of the Rh catalyst-electrode relative to the Pt electrode) rather than that of the individual Rh and Pt catalysts.

2. Experimental

2.1. YSZ solid electrolyte plates

The solid electrolyte plates provided by Bosch had a thickness of 0.25 mm and dimensions of 50 mm × 50 mm. They were made of yttria stabilized zirconia (YSZ, 8 wt.% Y_2O_3 with a resulting molar composition $Zr_{0.913}Y_{0.087}O_{1.957}$). The starting material had a mean particle size of 0.5 μm. The density in the sintered state was between 5.7 and 5.9 g/cm^3.

2.2. Sputter deposition and characterization of the Rh and Pt catalyst films

The 22 Rh/YSZ/Pt plates were prepared, as in Refs. [25,29] by metal sputtering at EPFL [25,29]. Prior to Rh or Pt deposition, no surface treatment was performed. The YSZ support was introduced into the sputtering chamber, filled with pure argon then metal (Rh 99.8 or Pt 99.99, Lesker) was deposited onto the substrate at 50 °C. The sputtering conditions were the following: direct current (dc) mode with a discharge of 350 V, argon pressure of 0.5 Pa. Under these conditions the deposition rate is 0.10–0.15 nm/s. The film thickness was measured by calibration with smooth silicon samples processed simultaneously. The thickness of the sputter-deposited rhodium and platinum films was 40 nm. The preparation and characterization procedure is identical to that used in [25,29] and, in fact, the 22 Rh/YSZ/Pt catalyst plates are the same ones used in [25,29] some four and two years ago, respectively. The excellent stability of these sputtered catalyst films prepared at EPFL [25,29] without any measurable loss of catalytic activity after prolonged exposure to rather severe operating conditions is particularly noteworthy and promising for practical applications.

The surface area of the Rh and Pt catalyst films, as well as the metal dispersion, was estimated using the galvanostatic transient technique, by measuring the time constant, τ, required for the rate increase, Δr, in galvanostatic electropromotion rate transients to reach 63% of its steady-state value [14]. In this way one can estimate the reactive oxygen uptake, N_G, of the anodically polarized metal film and, assuming a 1:1 surface metal:O ratio, the active catalyst surface area, N_G, expressed in mol, calculated by

$$N_G = \frac{I\tau}{2F} \quad (6)$$

during the current imposition [14] or by

$$N_G = \frac{r\tau_D}{\Lambda} \quad (7)$$

in the current interruption technique [14], where r is the electropromoted rate and the depolarization time, τ_D, expresses the average lifetime of the backspillover oxygen species originating from the YSZ lattice. These promoting $O^{\delta-}$ species are more strongly bonded to the catalytic surface than normally adsorbed oxygen [14].

These experiments were conducted both with anodic and cathodic polarization in an effort to estimate the surface area of both the Rh and Pt catalysts.

As in a previous study [30], the total surface area of the Rh catalysts per plate was estimated to be $(1.3–5.6) \times 10^{-6}$ mol Rh and $(1.8–4.3) \times 10^{-6}$ mol Pt. Since the metal loading per plate is of the order of 10^{-5} mol Rh or Pt, it follows that these thin (~40 nm) films are porous and mostly amorphous and that the Rh and Pt metal dispersions are of the order of 10–40%, i.e. comparable to that of commercial dispersed catalysts.

2.3. MEP reactor operation

The MEP reactor was placed in a tubular furnace and its temperature was measured and controlled by a type K thermocouple embedded in the metal casing at a distance of 1 mm from the gas entrance. The feed gas composition and total flow rate, F_v, was controlled by four mass flowmeters (Brooks smart mass flow and controller B5878). Reactants were Messer–Griesheim certified standards of C_2H_4 in He, O_2 in He and NO in He. Pure He (99.99%) was fed through the fourth flowmeter in order to further adjust total flow rate and inlet gas composition at desired levels. Reactants and products were analyzed by on-line gas chromatography (Varian 3800 equipped with a Porapak-Q column at 50 °C for the separation of C_2H_4, CO_2 and N_2O and a molecular sieve column at 70 °C for the separation of N_2 and O_2), in conjunction with an IR CO-CO_2 analyzer (Fuji Electric) and a chemiluminescence NO/NO_x analyzer (ECO Physics CLD 700 EL ht). Constant currents and potentials were applied using an AMEL 2053 galvanostat–potentiostat.

The oxygen excess (Π) is defined from:

$$\Pi = \left(y_{O_2} + \frac{y_{NO}}{2}\right) - 3y_{C_2H_4} \quad (8)$$

while mass balance dictates that the O_2 mol fraction in the reactor outlet stream corresponds to

$$y_{O_2}^{out} = \left(y_{O_2}^{in} + \frac{y_{NO}^{in} - y_{NO}^{out}}{2}\right) - 3(y_{C_2H_4}^{in} - y_{C_2H_4}^{out}) \quad (9)$$

Thus y_{O_2} varies in the MEP reactor from $y_{O_2}^{in}$ to $y_{O_2}^{out}$ and thus the local Π may decrease significantly downstream when $y_{O_2}^{out}$ is significantly smaller than $y_{O_2}^{in}$.

3. Results and discussion

Fig. 1 presents typical galvanostatic NEMCA experiments, showing, at five different temperatures, i.e. 240, 260, 280, 300 and 320 °C, the transient response of the NO reduction rate and conversion (a) of the CO_2 formation rate and of the conversion of C_2H_4 (b) and of the Rh–Pt potential difference (c) upon a constant applied anodic current (+30 mA). As shown, under anodic current application the maximum achieved NO conversion is *ca.* 94% at 280 °C, while C_2H_4 conversion reaches *ca.* 97% at 320 °C. Worth to note in Fig. 1 is the existence of a new, third steady state (SS3) after current interruption, close to the electropromoted steady state, obtained only at high temperatures (300 and 320 °C) and concomitant high conversions. At lower temperatures the catalytic reaction rates return reversibly to their initial open circuit values after current interruption.

Throughout this paper we denote as "third steady state" the permanent NEMCA steady state obtained after current interruption at high reactant conversion.

As shown in the figure, at 300 °C the NO and C_2H_4 conversion under open circuit conditions are 28 and 40%, respectively. Anodic current application causes a 3.4-fold increase in the conversion of NO reaching 95% and a 2.3-fold increase in the conversion of C_2H_4 reaching 90%. As also shown in the figure the apparent Faradaic efficiency for both NO reduction and CO_2 formation exceeds unity, indicating that electrochemical promotion and not pure electrocatalysis occurs. On the other hand negative polarization did not have any effect, positive or negative, on the reaction rate, confirming the overall electrophobic behaviour of the Rh/YSZ/Pt elements.

It is worth noting in Fig. 1 and subsequent figures that $|\Lambda_{NO}|$ is much smaller than $|\Lambda_{CO_2}|$, typically by a factor of 20–100. This is because, as in all previous studies of NO reduction on Rh or Pt metal

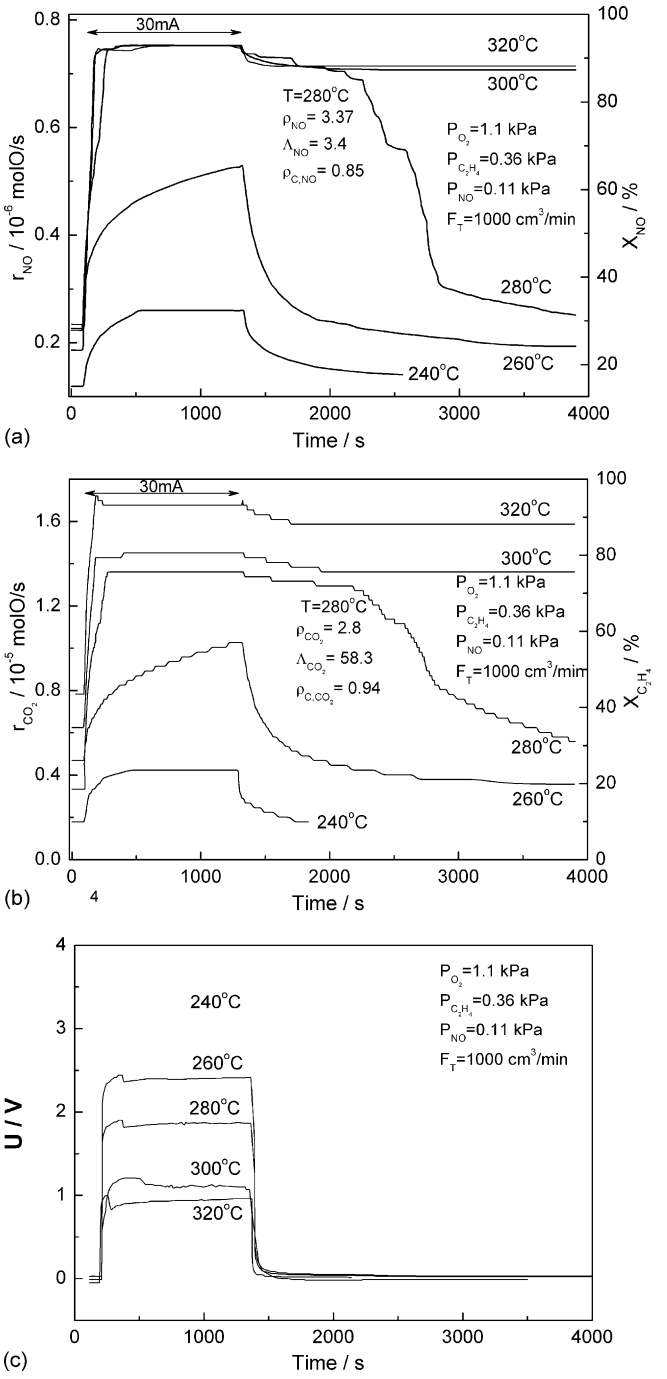

Fig. 1. Transient response of the NO reduction rate and conversion (a), of the CO_2 formation rate and C_2H_4 conversion (b) and of the Rh–Pt potential difference (c) upon a constant anodic current application (+30 mA) at different temperatures between 240 and 320 °C. Total volumetric flowrate F_T = 1 l/min.

catalysts, the normal catalytic rate of NO reduction, particularly under oxidizing conditions, is typically a factor of 20–100 smaller than the rate of hydrocarbon oxidation. This reflects the fact that the rate of NO reduction is intrinsically much slower than the rate of hydrocarbon oxidation on these catalytic metal surfaces. Typical turnover frequencies (TOFs) for NO reduction are 10^{-3} s^{-1} vs. 10^{-1} s^{-1} for hydrocarbon oxidation [14]. Thus, since the order of magnitude of $|\Lambda|$ can be estimated from [14]:

$$|\Lambda| = \frac{2Fr_o}{I_o} \quad (10)$$

where I_o is the exchange current of the catalyst/electrode in presence of the reacting mixture, one can rationalize immediately the observed large $|\Lambda|_{CO_2}/|\Lambda|_{NO}$ ratios.

The observed overall electrophobic behaviour, i.e. rate increase with potential, is similar to that obtained in previous electropromotion studies of NO reduction on Rh [14,30,32–34] and can be rationalized by accounting for the effect of decreasing strength of oxygen chemisorption on Rh with anodic polarization due to the repulsive lateral interactions with the spillover O^{2-} species. On the other hand the NO reduction on Pt under near-stoichiometric oxygen conditions is known [14,36] to exhibit electrophilic behaviour, due to weaker oxygen chemisorption [14,36] so that the effect seen in Fig. 1 and subsequent figures is the sum of the electropromotion effect of Rh (anodic polarization) and Pt (cathodic polarization). These two effects cannot be, unfortunately, separated in a MEPR with Rh/YSZ/Pt elements. Such a separation requires the use of more-or-less inert (e.g. Au) counter electrodes as is done in single chamber studies of the electropromotion of NO reduction [36–53].

Interestingly, as shown in Fig. 1 current interruption leads both the NO reduction and the CO_2 formation rate to the third steady state (SS3) where the NO and C_2H_4 conversions are 88 and 76%, respectively. The bifurcation point between reversible and irreversible (permanent) NEMCA behaviour appears to be near 280 °C where the catalytic rates return to their initial values but only after a long time period.

As shown in Fig. 1(c), at temperatures ≥260 °C, a few seconds after current application the Rh–Pt potential difference exhibits a more complex transient, i.e. a sharp transient decrease, which is related to a surface phase transition of the Rh catalyst-electrode. Such behaviour is similar to that obtained in previous electropromotion studies of NO reduction on Rh [30,51,52] and can be attributed to a change in the oxidation state of the catalyst, i.e. the reduction of the surface Rh_2O_3 phase, via positive polarization. This behaviour is quite common when the catalyst surface is initially oxidized (i.e. has a very high oxygen coverage, very likely forming an ordered monolayer surface Rh_2O_3 phase) [30]. The destruction of this phase via anodic polarization has been attributed [14] to the lateral repulsive interactions caused between the backspillover $O^{\delta-}$ ionic species from the electrolyte and the O species of the Rh oxide surface film, which destroy the Rh surface oxide film and results in the observed decrease of the Rh–Pt potential difference and concomitant increase of the catalytic rate. When the partial pressure of O_2 above the Rh catalyst film is higher than a critical P_{O_2} value, then anodic polarization is not sufficient to destroy the surface Rh_2O_3 phase and thus the catalytic rates remain low [14,54,55]. On the other hand when P_{O_2} is low the surface Rh_2O_3 phase does not form at all [14,54,55]. These considerations play an important role in the present case of the MEP reactor under near-stoichiometric conditions, since at higher temperatures and under electropromotion conditions the conversion of O_2 is quite high.

Thus a rationalization of the origin of this high conversion steady state (SS3), is that since it appears only at high O_2 conversion, it corresponds to the high conversion steady states that appear in catalytic reactors with some backmixing where the kinetics are complex (e.g. Langmuir–Hinshelwood type kinetics), as in the case of CO oxidation over Pt catalysts [56,57]. In such reaction systems there are three steady states; the low conversion one is stable, followed by a second unstable state and by a third stable state, characterized by high conversion. In the present study the initial open circuit state corresponds to the first (low conversion, high P_{O_2}) stable steady state, while the one after the current interruption (SS3) corresponds to the third (high conversion, low P_{O_2}) stable, steady state.

Thus a difference between the SS3 state obtained here and classical permanent NEMCA states [4,34,35] is that in the latter case the gas composition (more specifically the P_{O_2} value) in contact with the catalyst does not change appreciably during electropromotion while in the present case, due to the high conversions in the MEPR, the P_{O_2} value in contact with the catalyst changes very significantly. Therefore in the present case the observed steady-state multiplicity and the appearance of SS3 is the result of the synergistic action of the high conversion reactor and the electropromoted catalyst while in classical permanent NEMCA studies [4,34,35] it is the result of the electropromoted catalyst alone.

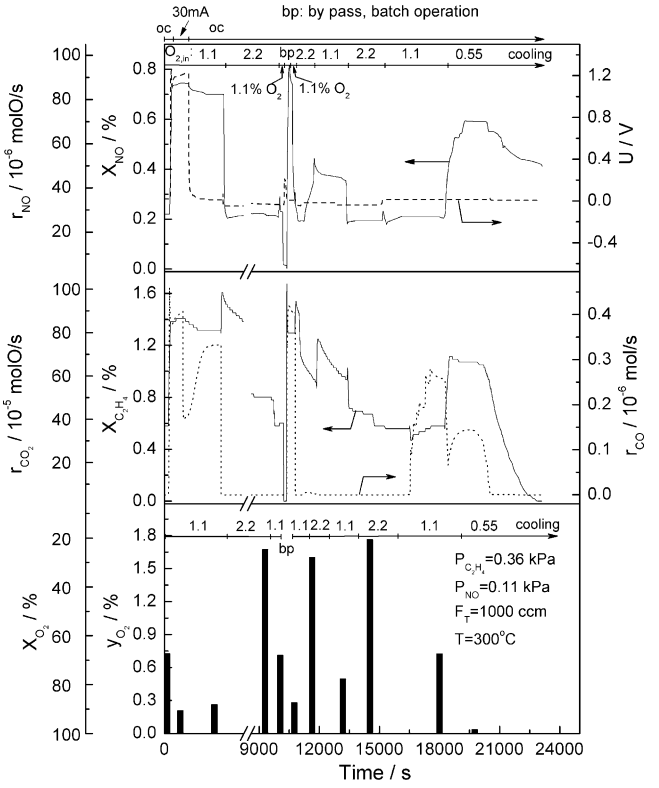

Fig. 2. Transient effect of a constant applied anodic current (+30 mA) and of imposed changes in the feed mole fraction of O_2 concentration in the feed gas mixture on the NO reduction rate and NO conversion, on the CO_2 formation rate and C_2H_4 conversion, on the O_2 concentration in the outlet of the reactor, on the O_2 conversion, on the Rh–Pt potential difference and on the CO production rate. Total volumetric flowrate F_T = 1 l/min, T = 300 °C.

Fig. 2 shows the transient effect of several O_2 feed concentration changes on the NO reduction rate and NO conversion, on the CO_2 and CO formation rates, on the conversion of C_2H_4, and on the Rh–Pt potential difference, under open circuit and anodic polarization conditions, at 300 °C and under 1 l/min gas flow rate.

As shown, initially an anodic current (+30 mA) was applied in order to increase the reaction rates from the initial open circuit to the electropromoted steady state. As already discussed (Fig. 1), current interruption leads under these conditions to the third steady state (SS3). At this steady state the O_2 concentration in the outlet of the reactor is *ca.* 0.3%, i.e. 73% conversion of O_2 has obtained. In addition, at the electropromoted and the SS3 steady state some CO formation takes place, due to the low O_2 concentration in the reactor. The CO formation rate is approximately two orders of magnitude smaller than the corresponding CO_2 formation rate, which is quite typical of C_2H_4 oxidation on Rh and Pt catalysts in this temperature range [14].

Increase of the O_2 concentration in the feed to 2.2%, under constant total gas flow rate (1 l/min) causes a sudden decrease of the NO reduction rate at values slightly lower than those obtained at the initial open circuit state (1.1% O_2). This sudden decrease of

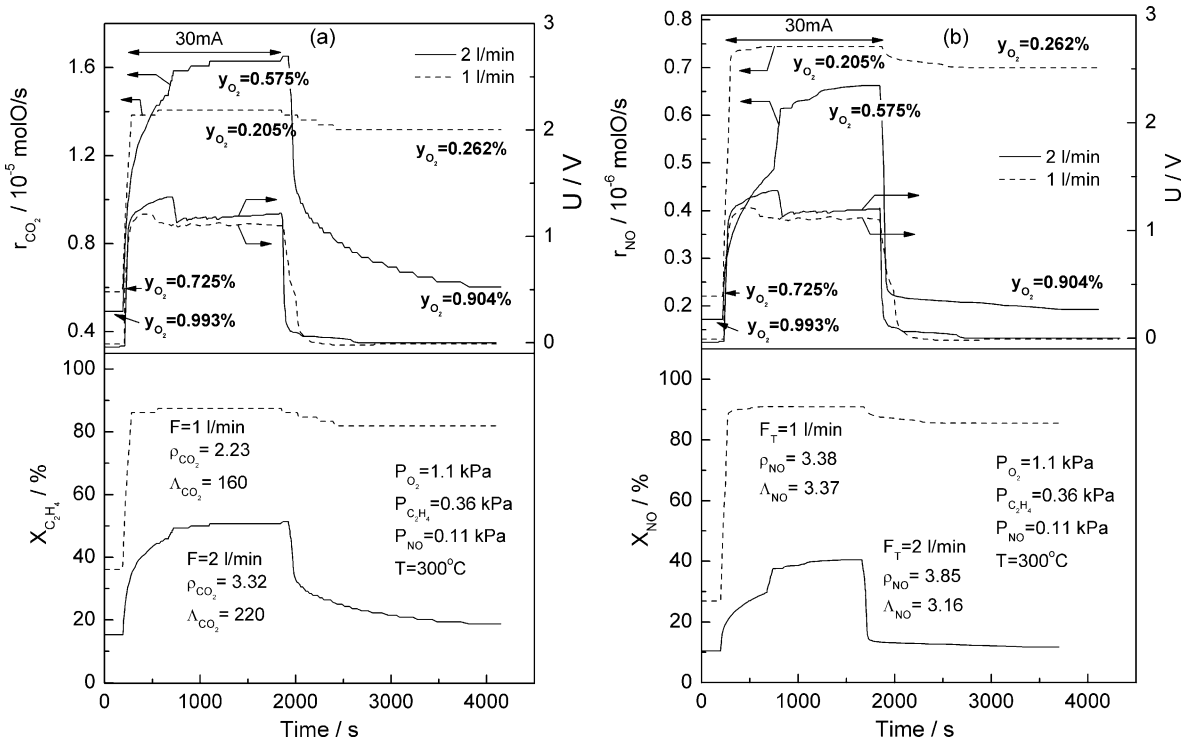

Fig. 3. Transient effect of a constant applied current (+30 mA) on the CO_2 formation rate on the exit, O_2 mole fraction and on the C_2H_4 conversion (a), on the NO reduction rate and NO conversion (b) and on the Rh–Pt potential difference. T = 300 °C.

NO reduction rate is in contrast to the slow decrease of the CO_2 formation rate, indicating that NO reduction is very sensitive to P_{O_2} [21,24] and occurs mainly on Rh (as also manifested by the observed high selectivity to N_2) while C_2H_4 oxidation occurs both on Rh and on Pt, where it is much less sensitive to P_{O_2} [14,30,31].

The observed transient increase of CO_2 formation rate and decrease of NO reduction rate with 2.2% O_2 compared to those under 1.1% O_2, can be attributed to the fact that CO_2 formation on Pt is favored by O_2 excess [14], while NO reduction on Rh is, severely poisoned by O_2 in high excess O_2, as already discussed. Decrease of the O_2 feed mole fraction to the initial 1.1% value causes the NO reduction and CO_2 formation catalytic rates to return to their initial values, i.e. those obtained before the anodic current application.

Another way to increase the reactant conversion close to that in the electropromoted state and to force the system to remain in the SS3 state, is to operate the reactor in a batch mode, with an operation time greater than that in the CSTR-type mode (0.04 s).

Thus, batch operation mode for 15 s and return to the continuous flow operation leads the system to the third steady state (SS3), exactly as in the case of anodic polarization and current interruption. This can be rationalized by taking into account that during the batch operation the reactants conversions reach values close to full conversion (as in the electropromoted steady state), decreasing close to zero the O_2 concentration in the mixture. Hence, the return to the continuous flow mode leads the system to the state SS3. Consequently, the electropromotion and the batch-type operation constitute two different ways for the increase of the reaction rates from the initial, low conversion open circuit state to the high conversion open circuit steady state (SS3) by reducing substantially the partial pressure of O_2.

Increase of the O_2 concentration at 2.2% just for ~15 min makes the reaction rates to decrease down to an intermediate steady state, which lies between the mentioned two open circuit steady states. This steady state seems to be unstable, as inferred from the slow decrease of the NO reduction and CO_2 formation rates, towards the initial open circuit steady-state values. A further step imposition of 2.2% O_2 concentration for ~20 min and then return at 1.1% O_2, leads the catalytic rates faster at the initial open circuit steady-state values.

On the other hand reduction of the feed O_2 concentration to 0.55% (overall reducing conditions) causes a great increase in the NO reduction and CO_2 formation catalytic rates and almost full conversion of the co-fed O_2.

Fig. 3(a) and (b) shows the transient effect of a constant applied anodic current (+30 mA) on the CO_2 formation (a) and NO reduction (b) catalytic rates, on C_2H_4 (a) and NO (b) conversions and on the Rh–Pt potential difference, under 1 and 2 l/min total gas flow rate at 300 °C. As discussed in the previous figures (Figs. 1 and 2), under 1 l/min total gas flow rate the catalytic reaction rates (NO reduction and CO_2 formation) increase significantly by anodic current imposition and after the current interruption remain in the state SS3. Under 2 l/min gas flow rate, initially, the NO conversion is ~10% and the C_2H_4 conversion is ~15%. Anodic current application leads to a significant increase of both reaction rates. The NO conversion reaches ~39%, enhanced by 285% (ρ = 3.85) while the C_2H_4 conversion reaches 50% enhanced by 230% (ρ = 3.32). The apparent Faradaic efficiency is 3.2 and 220, respectively, for the NO reduction and CO_2 formation reaction. The above two orders of magnitude difference between the Λ_{NO} and Λ_{CO_2} values is predicted by Eq. (8), since under open circuit conditions the CO_2 formation rate is almost two orders of magnitude larger than the NO reduction rate. By current interruption the NO reduction and CO_2 formation catalytic rates return to their initial values, without the existence of any new steady state, indicating the reversibility of the EPOC effect.

There are three main points to focus on in Fig. 3. First, by current interruption under 2 l/min flow rate, no high conversion steady state is reached, contrary to the 1 l/min case. Second, the electropromoted rate of CO_2 formation under 2 l/min gas flow rate is larger than that under 1 l/min, while the opposite is observed for the NO reduction rate. Third, under 2 l/min during the

first seconds of polarization, sharp changes of the reaction rates are observed, accompanied by sharp changes in the Rh–Pt potential difference.

The observed reversibility of the reaction rates after current interruption, under 2 l/min gas flow rate can be rationalized by accounting for the fact that in this case of O_2 conversion never exceeds 50% and thus y_{O_2} never decreases below 0.55%.

Under open circuit conditions, increase of the flow rate from 1 to 2 l/min, does not have any pronounced effect on the reaction rates. However, under anodic polarization conditions, an increase of the CO_2 formation rate and simultaneously a decrease of the NO reduction rate are observed, as the flow rate increases from 1 to 2 l/min. The above differences can the attributed to the relatively high O_2 concentration which remains in the reactor during reaction at 2 l/min. In detail, under open circuit conditions and 1 l/min gas flow rate, the C_2H_4 conversion is 37%, while under 2 l/min 17%. Similarly, the NO conversion decreases from 28% under 1 l/min to 10% under 2 l/min, almost a 3-fold decrease. However, under polarization conditions (+30 mA) the increase of the flow rate from 1 to 2 l/min, causes the decrease of C_2H_4 conversion from 90 to 51% and of NO from 93 to 40%.The above decrease of NO and C_2H_4 conversion is accompanied by a significant decrease of the O_2 conversion and thus, increase of the remaining O_2 concentration inside the reactor. Specifically, in open circuit state, P_{O_2} increases from 0.72 to 0.99%, while under anodic polarization conditions form 0.2 to 0.57%, as gas flow rate increases from 1 to 2 l/min, at 300 °C.

For the NO reduction by hydrocarbons reaction in presence of O_2, the O_2 excess is a parameter of major importance, as already discussed, and as shown by previous studies, there is a critical value of P_{O_2} ($P^*_{O_2}$), where at $P_{O_2} > P^*_{O_2}$ the NO reduction catalytic rate over Rh catalysts decreases significantly, due to formation of a surface Rh_2O_3 film, which is poisoning the reaction [14]. Hence, the observed drop of NO conversion is greater than the corresponding C_2H_4 conversion, leading to decrease of the NO reduction catalytic rate and increase of the CO_2 formation (C_2H_4 combustion) catalytic rate upon gas flow rate duplication.

Similar to Fig. 1(c), under 2 l/min total gas flow rate where it is more obvious, few seconds after the current application the Rh–Pt potential difference exhibits a more complex transient, i.e. a sharp decrease, related to phase transition of the Rh catalyst-electrode, accompanied by a sharp increase of the observed NO reduction and CO_2 formation catalytic rate. Such behaviour is similar to that obtained in previous electropromotion studies of NO reduction on Rh [30,51,52] and manifests a change in the oxidation state of the catalyst, i.e. reduction of the surface Rh_2O_3 phase.

Fig. 4 shows the transient effect of a constant applied anodic and cathodic current on the NO and C_2H_4 conversion, on the NO reduction and CO_2 formation catalytic rates, on the CO formation catalytic rate and on the Rh–Pt potential difference, under 1 l/min at 320 °C. As shown, initially, i.e. under open circuit conditions, NO and C_2H_4 conversions are 29 and 48%, respectively. Anodic current imposition causes a 5.3-fold increase of the NO conversion reaching 92% and a 2.1-fold increase of the C_2H_4 conversion reaching ~100%. Since, in the electropromoted state the reactants conversions are close to full conversion, ρ_c values are close to unity. Furthermore, the apparent Faradaic efficiency values, as shown in Fig. 4, are greater than unity ($\Lambda_{NO} = 3.2$, $\Lambda_{CO_2} = 54$) indicating that electrochemical promotion occurs and not pure electrocatalysis. Small quantities of CO were also detected under current application, possibly due to the low remaining O_2 concentration. Current interruption makes the reaction rates, as already shown in Fig. 1, to lie in the SS3 state where NO, C_2H_4 and O_2 conversions are 85, 91 and 86%, respectively.

Cathodic polarization (−30 mA) (i.e. negative Rh electrode and positive Pt electrode) has no effect on the NO reduction rate and only a minor positive effect on the CO_2 formation rate. This is in agreement with previous studies on Rh and Pt [14,30,31], which have shown that the reduction of NO by C_2H_4 in presence of O_2 is electropromoted significantly only when the Rh electrode is made positive and Pt electrode negative (electrophobic and electrophilic behaviour, respectively) [14].

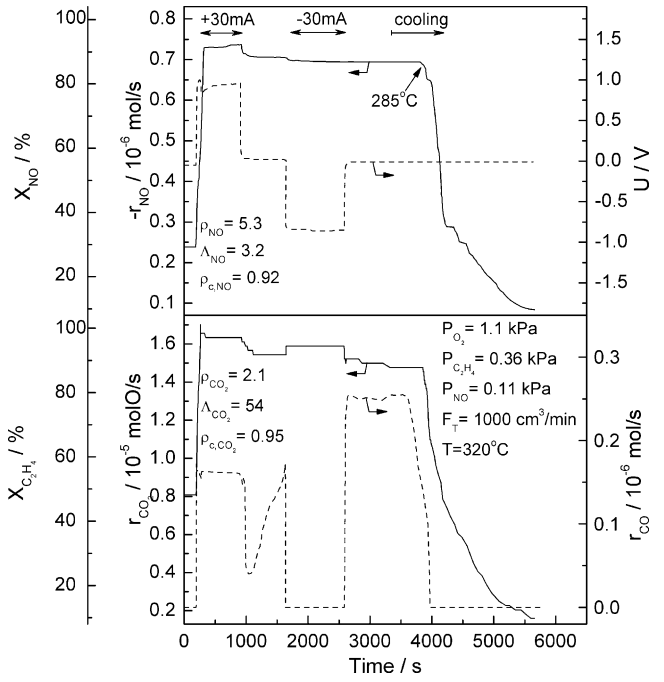

Fig. 4. Transient response of the NO reduction and the CO_2 formation rates, of the NO and C_2H_4 conversion, of the CO formation rate and of the Rh–Pt potential difference upon a constant anodic and cathodic current imposition. F_T = 1 l/min, T = 320 °C.

When the system lies at the SS3 state, temperature reduction (Fig. 4) has initially a small effect due to the reaction kinetics. Further decrease of the temperature below 290 °C leads to a sudden drop of the catalytic rates, i.e. a shift of the system from SS3 to the corresponding on temperature low conversion steady state. This is in agreement with the observations in Fig. 1.

As already shown in Fig. 3 an increase in total flowrate from 1 to 2 l/min causes the disappearance of SS3 at 300 °C. In order to show that indeed the SS3 state can also be observed at high flowrates (2 l/min) and thus its appearance depends only on the O_2 conversion and average P_{O_2} value in the reactor, and not on temperature or flowrate alone, we performed similar experiments at 2 l/min and higher temperatures, i.e. T = 340 °C (Fig. 5).

Thus Fig. 5 shows the transient effect of a constant applied anodic current (+30 mA) and of O_2 partial pressure changes on the NO and C_2H_4 conversion, on the NO reduction, on the CO_2 and CO formation catalytic rates and on the Rh–Pt potential difference, under 2 l/min total gas flow rate at 340 °C. As shown, at 340, 20 °C higher that the maximum examined temperature in Fig. 1, and under 2 l/min total gas flow rate, initially NO conversion is ~24% and C_2H_4 conversion ~60%. By anodic current application (+30 mA), NO conversion reaches ~82% and C_2H_4 conversion ~95%. The rate enhancement ratio for the NO reduction and CO_2 formation reactions were 3.6 and 1.7, respectively, while the apparent Faradaic efficiency was found to be greater than unity for both reactions ($\Lambda_{NO} = 5.7$ and $\Lambda_{CO_2} = 107$), indicating that EPOC occurs even under high gas flow rates and temperatures. In this case also, there is a two orders of magnitude difference between the apparent Faradaic efficiency of NO reduction and CO_2 formation reactions which can be rationalized by accounting for

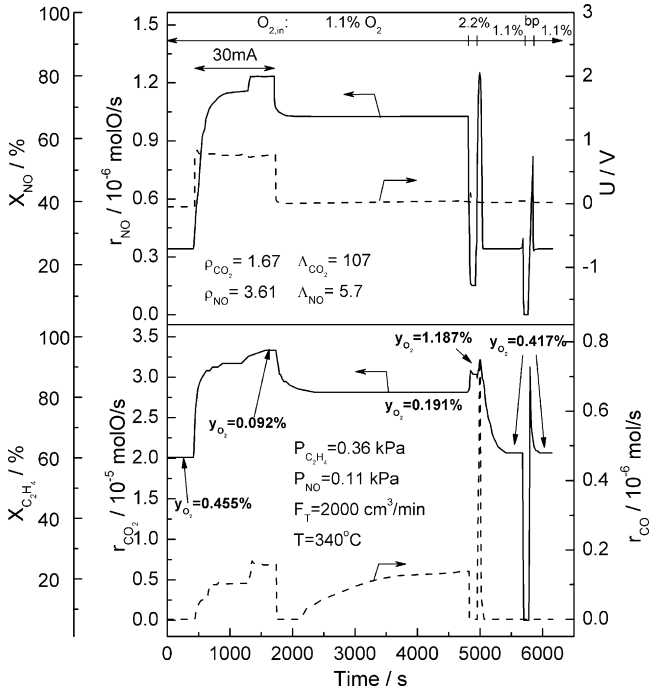

Fig. 5. Transient effect of a constant applied current and of imposed changes in the feed mole fraction of O_2, on the NO reduction and CO_2 formation rates, on the conversion of NO and C_2H_4, on the CO formation rate and on the Rh–Pt potential difference. F_T = 2 l/min, T = 340 °C.

the initial, i.e. normal catalytic rate of each reaction in combination with Eq. (8) [14].

By current interruption, the Rh–Pt potential difference returns to its initial value, while the catalytic rate lies in a new high conversion steady state, similar to the one discussed above (Figs. 1–4) under 1 l/min and that at 300 and 320 °C. In Fig. 3(a and b) where the effect of anodic polarization under 2 l/min flow rate was examined at lower temperature (300 °C), no evidence of the SS3 was found. Thus, the higher temperature and concomitant increase in reaction rates counterbalances the higher flowrate and thus leads again to the appearance of the SS3 state even at 2 l/min flowrate. Increase of the feed O_2 concentration to 2.2% causes, in this case too, the shift of the reaction rates from SS3 to the initial open circuit steady state. Thus Fig. 5 shows that the appearance of SS3 is not dictated by temperature or flowrate alone but by the high conversion of O_2 in the reactor leading to $P_{O_2} < P^*_{O_2}$ and thus to the stabilization of the highly active reduced Rh catalyst phase.

4. Conclusions

A monolithic electrochemically promoted reactor equipped with 22 Rh/YSZ/Pt-plates was used for the reduction of NO by C_2H_4 under mildly oxidizing conditions at temperatures from 240 to 340 °C and under 1 and 2 l/min total gas flow rate. It was found that significant electropromotion takes place for both the NO reduction and the CO_2 formation, leading to NO and fuel conversions up to 95 and 100%, respectively. Also, it was found that there are two stable steady states under open circuit conditions, one inactive and one, obtained via previous anodic polarization, which is highly active and selective. The appearance of this highly active permanent NEMCA state appears to be due to the significant reduction of the gaseous O_2 concentration during anodic polarization and indicates some extent of backmixing in the reactor. This high conversion state may be useful for practical applications.

For such applications a thorough understanding of possible temperature and concentration gradients in the MEP reactor becomes necessary. In the present case the two thermocouples before and after the reactor showed only minor (2–3 °C) differences so that the actual temperature profile in the MEPR was apparently rather flat and dictated by the heating furnace rather than by the exothermicity of the oxidation reaction. On the other hand the axial concentration gradient of O_2 was quite pronounced (near complete conversion) and is, as already discussed, beneficial and intimately related to the appearance of the highly active state SS3. Although such axial concentration gradients can be quite beneficial, the onset of concentration gradients for the gas stream to the catalyst surface (mass transfer limitations) can have a detrimental effect, since at the limit of complete mass transfer limitations (very high Carberry or Damköhler numbers) there can by definition be no electropromotion. The strong electropromotion obtained in the present study indicates that mass transport limitations were not dominant. However, one cannot exclude the possibility of some mass transport limitations of the maximum observed electropromoted rates. The experimental and theoretical study of such mass and heat transfer limitations in MEP reactors can be quite fruitful for enhancing the possibilities of their eventual practical utilization.

References

[1] C.G. Vayenas, S. Bebelis, S. Ladas, Nature 343 (1990) 625.
[2] J. Pritchard, Nature 343 (1990) 592.
[3] R.M. Lambert, F. Williams, A. Palermo, M.S. Tikhov, Top. Catal. 13 (2000) 91.
[4] G. Foti, S. Wodiunig, C. Comninellis, Curr. Top. Electrochem. 7 (2000) 1.
[5] C.A. Cavalca, G.L. Haller, J. Catal. 177 (1998) 389.
[6] L. Ploense, M. Salazar, B. Gurau, E.S. Smotkin, J. Am. Ceram. Soc. 119 (1997) 11550.
[7] P. Vernoux, F. Gaillard, L. Bultel, E. Siebert, M. Primet, J. Catal. 208 (2002) 412.
[8] I. Metcalfe, J. Catal. 199 (2001) 247.
[9] C. Sanchez, E. Leiva, in: W. Vielstich, H. Gasteiger, A. Lamm (Eds.), Handbook of Fuel Cells: Fundamentals, Technology and Applications, vol. 2, Wiley, UK, 2003.
[10] G.-Q. Lu, A. Wieckowski, Curr. Opin. Colloid Interface Sci. 5 (2000) 95.
[11] B. Grzybowska-Swierkosz, J. Haber, Annual Reports on the Progress of Chemistry, The Royal Society of Chemistry, Cambridge, 1994.
[12] J.O.M. Bockris, Z.S. Minevski, Electrochim. Acta 39 (1994) 1471.
[13] C.G. Vayenas, M.M. Jaksic, S. Bebelis, S.G. Neophytides, in: J.O.M. Bockris, B.E. Conway, R.E. White (Eds.), Modern Aspects of Electrochemistry, vol. 29, Kluwer Academic Publishers/Plenum Press, New York, 1996, p. 57.
[14] C.G. Vayenas, S. Bebelis, C. Pliangos, S. Brosda, D. Tsiplakides, Electrochemical Activation of Catalysis: Promotion, Electrochemical Promotion and Metal-Support Interactions, Kluwer Academic Publishers/Plenum Press, New York, 2001 (and references therein).
[15] A. Wieckowski, E. Savinova, C.G. Vayenas, Catalysis and Electrocatalysis at Nanoparticles, Marcel Dekker, New York, 2003.
[16] J. Nicole, D. Tsiplakides, C. Pliangos, X.E. Verykios, C. Comninellis, C.G. Vayenas, J. Catal. 204 (2001) 23.
[17] X.E. Verykios, in: A. Wieckowski, E.R. Savinova, C.G. Vayenas (Eds.), Catalysis and Electrocatalysis at Nanoparticles Surfaces, Marcel Dekker, New York, 2003.
[18] M.D. Amiridis, T. Zhang, R.J. Farrauto, Appl. Catal. B 10 (1996) 203.
[19] A. Fritz, V. Pitchon, Appl. Catal. B 13 (1997) 1.
[20] V.I. Parvulescu, P. Grange, B. Delmon, Catal. Today 46 (1998) 233.
[21] T.I. Halkides, D.I. Kondarides, X.E. Verykios, Catal. Today 73 (2002) 213.
[22] T. Chafik, D.I. Kondarides, X.E. Verykios, J. Catal. 190 (2000) 446.
[23] T. Chafik, A.M. Efstathiou, X.E. Verykios, J. Phys. Chem. B 101 (1997) 7968.
[24] D.I. Kondarides, T. Chafik, X.E. Verykios, J. Catal. 191 (2000) 147.
[25] S.P. Balomenou, D. Tsiplakides, A. Katsaounis, S. Thiemann-Handler, B. Cramer, G. Foti, Ch. Comninellis, C.G. Vayenas, Appl. Catal. B 52 (2004) 181.
[26] D. Tsiplakides, S. Balomenou, A. Katsaounis, D. Archonta, C. Koutsodontis, C.G. Vayenas, Catal. Today 100 (2005) 133.
[27] S.P. Balomenou, D. Tsiplakides, A. Katsaounis, S. Brosda, A. Hammad, G. Foti, Ch. Comninellis, S. Thiemann-Handler, B. Cramer, C.G. Vayenas, Solid State Ionics 171 (2006) 2201.
[28] S. Balomenou, D. Tsiplakides, C.G. Vayenas, S. Poulston, V. Houel, P. Collier, A. Konstandopoulos, Ch. Agrafiotis, Top. Catal. 44 (3) (2007) 481.
[29] C. Koutsodontis, A. Hammad, M. Lepage, Y. Sakamoto, G. Foti, C.G. Vayenas, Top. Catal. 50 (1–4) (2008) 191.
[30] S. Souentie, A. Hammad, S. Brosda, G. Foti, C.G. Vayenas, J. Appl. Electrochem. 38 (2008) 1159.
[31] C.G. Vayenas, S. Brosda, C. Pliangos, J. Catal. 203 (2001) 329.
[32] C. Pliangos, C. Raptis, T. Badas, C.G. Vayenas, Solid State Ionics, 136/137 (2000) 767.
[33] M. Marwood, A. Kaloyannis, C.G. Vayenas, Ionics 2 (1996) 302.
[34] G. Foti, O. Lavanchy, Ch. Comninellis, J. Appl. Electrochem. 30 (2000) 1223.
[35] C. Falgairete, A. Jaccoud, G. Foti, Ch. Comninellis, J. Appl. Electrochem. 38 (2008) 1075.
[36] C. Pliangos, C. Raptis, Th. Badas, C.G. Vayenas, Ionics 6 (2000) 119.

[37] C. Pliangos, C. Raptis, Th. Badas, D. Tsiplakides, C.G. Vayenas, Electrochim. Acta 46 (2000) 331.
[38] B. Beguin, F. Gaillard, M. Primet, P. Vernoux, L. Bultel, M. Henault, C. Roux, E. Siebert, Ionics 8 (2002) 128.
[39] P. Vernoux, F. Gaillard, R. Karoum, A. Billard, Appl. Catal. B 73 (2007) 73.
[40] M. Marwood, C.G. Vayenas, J. Catal. 170 (1997) 275.
[41] S. Kim, G.H. Haller, Solid State Ionics 136 (137) (2000) 693.
[42] F.J. Williams, N. Macleod, M.S. Tikhov, R.M. Lambert, Electrochim. Acta 47 (2002) 1259.
[43] I.R. Harkness, R.M. Lambert, J. Catal. 152 (1995) 211.
[44] A. Palermo, R.M. Lambert, I.R. Harkness, I. Yentekakis, O. Marina, C.G. Vayenas, J. Catal. 161 (1996) 471.
[45] O.A. Marina, I.V. Yentekakis, C.G. Vayenas, A. Palermo, R.M. Lambert, J. Catal. 166 (1997) 218.
[46] I.V. Yentekakis, A. Palermo, N.C. Filkin, M.S. Tikhov, R.M. Lambert, J. Phys. Chem. B 101 (1997) 3759.
[47] F. Dorado, A. de Lucas-Consuegra, C. Jimenez, J.L. Valverde, Appl. Catal. A 321 (2007) 86.
[48] F. Dorado, A. de Lucas-Consuegra, P. Vernoux, J.L. Valverde, Appl. Catal. B 73 (2007) 42.
[49] R.M. Lambert, A. Palermo, F.J. Williams, M.S. Tikhov, Solid State Ionics 136 (137) (2000) 677.
[50] F.J. Williams, M.S. Tikhov, A. Palermo, N. Macleod, R.M. Lambert, J. Phys. Chem. B 105 (2001) 2800.
[51] F.J. Williams, A. Palermo, M.S. Tikhov, R.M. Lambert, Surf. Sci. 482 (2001) 177.
[52] P. Vernoux, F. Gaillard, C. Lopez, E. Siebert, J. Catal. 217 (2003) 203.
[53] I. Constantinou, D. Archonta, S. Brosda, M. Lepage, Y. Sakamoto, C.G. Vayenas, J. Catal. 251 (2007) 400.
[54] E.A. Baranova, A. Thursfield, S. Brosda, G. Foti, Ch. Comninellis, C.G. Vayenas, J. Electrochem. Soc. 152 (2) (2005) E40.
[55] J. Nicole, D. Tsiplakides, C. Pliangos, X.E. Verykios, Ch. Comninellis, C.G. Vayenas, J. Catal. 204 (2001) 23.
[56] I. Chorkendorff, J.W. Niemantsverdriet, Concepts of Modern Catalysis and Kinetics, Wiley-VCH Verlag GmbH & Co. KGaA, Weinheim, 2003.
[57] L.D. Schmidt, The Engineering of Chemical Reactions (Topics in Chemical Engineering), Oxford University Press, Inc., New York, 1998.